Effect of Contact Spacing on Efficiency of Flat-Plate Solar Collectors

S. Crha* and G.E. Schneider†
University of Waterloo, Ontario, Canada

The attachment of an extended surface to an energy removal tube in a noncontinuous manner is considered. Rather than to provide continuous weld or solder to form thermal contact, the use of a uniform distribution of finite regions of contact is examined. In particular, the application to solar energy collection is considered where a discrete, discontinuous system of contacts offers potential economic benefit in the fabrication and reliability aspects of construction. The problem is formulated mathematically in nondimensional terms and numerical solutions employing the finite element method are obtained. Specifically, the sensitivity of the thermal performance of the collector system to weld/solder joint dimensions is presented. It is found that the discontinuous nature of the weld can significantly degrade system performance with the degree of degradation strongly dependent on the fin surface Biot modulus. Further, it is observed that the controlling parameter with respect to the weld dimensions is the perimeter length of the weld location of contact. This observation will permit direct application of the results obtained to situations other than the rectangular weld planform specifically considered. A novel and useful method of representation, in the form of a relative performance ratio, is also introduced and should prove useful in future two-dimensional fin analyses.

Nomenclature

a,b,c,d,e	= dimensions of fin problem (Fig. 2)
A	= area
Bi	= Biot modulus, $=ht/k$
h	= heat-transfer coefficient
k	= thermal conductivity
q	= incident radiative flux
RPR	= relative performance ratio
t	= thickness
T	= temperature
x,y	= Cartesian coordinates
$\alpha,\beta,\gamma,\delta,\zeta$	= nondimensional fin dimensions (Fig. 3)
η	= efficiency
θ	= nondimensional temperature
κ	= conductivity-thickness parameter, $\equiv k_f t_f/k_p t_p$
ϕ	= one-dimensional parameter, $\equiv \beta^2 Bi_f/t_f^{*2}$

Subscripts

f	= fin
p	= pipe
s	= sol-air designation
$1,2,c$	= fin, pipe, and contact region temperatures, respectively

Superscripts

$()^*$	= nondimensional quantity

Introduction

IN heat exchanger configurations it is common practice to employ tube passages for energy removal that are fastened to the wall of an exchanger surface which, in turn, is exposed to a radiant flux as well as a second fluid which convectively interacts with this surface. If continuous contact of the tubes to the wall is made along the tube length, a one-dimensional analysis can be performed to determine the operational characteristics. However, if thermal contact is made between the tube and the wall only at regular intervals, the analysis becomes two-dimensional. For this two-dimensional problem, performance characteristics are not available since this problem has not yet been investigated.

With particular reference to flat-plate solar collector energy removal, there are significant cost benefits that can accrue from the use of a regular thermal contact pattern (i.e., solder or weld locations) rather than employing a continuous solder or weld attachment along the entire tube length. However, as the collector-plate temperature significantly affects the efficiency of energy collection, and the thermal tube/plate contact will affect the collector-plate temperature, it is imperative that the performance characteristics of an energy removal system utilizing such a regularized contact pattern be thoroughly understood. Only then can significant steps be taken in proposing contact distributions that will permit unit cost reductions without significantly affecting the system energy collection efficiency.

The purpose of the proposed paper is to examine such a system and to determine the performance characteristics relevant to system design and construction. The system being examined is shown schematically in Fig. 1, where a typical analysis section has been selected for examination on the basis of symmetry considerations. While the basic problem bears a strong resemblance to the contact problems encountered in heat exchanger analysis and other applications,[1-4] the problem is, nevertheless, quite unique in that there is convective and radiative exposure to the environment throughout the entire domain. Thermal contact between the collector-plate fin and energy removal tubes is assumed to exist only over the area in which the weld or solder application has been made. This represents a conservative, worst-case scenario since, if contact is made at other locations due to intermittent mechanical contact or by convection, the collection efficiency will be higher than that corresponding to the proposed model configuration. However, since the contact at the weld locations is thermally much superior to that other locations due to mechanical contacts and local convection, the proposed model is indeed highly representative of the expected conditions and quite realistic from a modeling

Presented as Paper 84-0146 at the AIAA 22nd Aerospace Sciences Meeting, Reno, NV, Jan. 9-12, 1984; submitted March 1, 1984; revision submitted Oct. 5, 1984. This paper is declared a work of the Canadian Government and therefore is in the public domain.

*Graduate Student, Thermal Engineering Group, Department of Mechanical Engineering.

†Professor, Thermal Engineering Group, Department of Mechanical Engineering. Member AIAA.

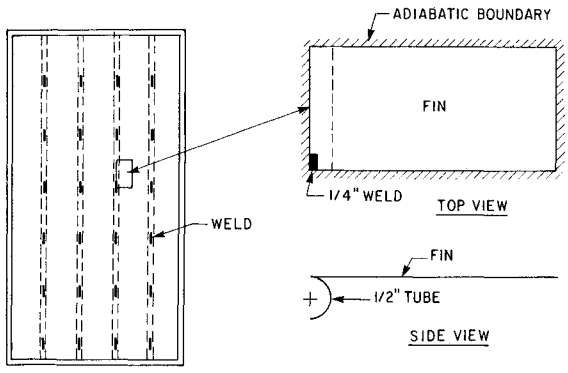

Fig. 1 Physical problem configuration.

point of view. For purposes of modeling the tube energy transfer, however, the tube curvature effects are neglected and conduction is modeled as occurring in a rectangular plate of tube wall thickness and size given by the tube wall mean radius surface area. The fin assumption is employed for both the collector and the tube component of the analysis cell. The above-described problem has not been addressed previously and it is the purpose of this paper to examine the influence of problem parameters on the energy collection efficiency. In particular, the influence of the weld dimensions on collection efficiency is of vital interest.

Mathematical Formulation of the Problem

The components of the analysis geometry are shown in Fig. 2. Convection couples the top surface of the collector fin portion, designated by the subscript f, to an ambient fluid at temperature T_f. In addition, a radiant flux is incident on the top surface of the collector plate, and, indeed, represents the energy for which collection is desired. The lower inner surface of the energy removal piping, designated by the subscript p, is convectively coupled to the energy collection fluid at local temperature T_p. The lower surface of the collector plate is insulated as is the upper surface of the energy removal piping. The weld area is modeled as a region of rectangular cross section, as shown in the plan view of Fig. 2, with the fin and piping being in intimate contact only over this region.

Both the fin material and energy removal piping are modeled using the fin assumption; i.e., temperature gradients across the material thickness are neglected. An energy balance, in the steady state, performed on a differential element $dx \cdot dy$, results in the equation

$$\frac{\partial}{\partial x}\left(k_f t_f \frac{\partial T_1}{\partial x}\right) + \left(\frac{\partial}{\partial y} k_f t_f \frac{\partial T_1}{\partial y}\right) - h_f(T_1 - T_f) + \alpha q = 0 \tag{1}$$

Introducing the definition of a sol-air temperature, defined by

$$T_s \equiv T_f + \alpha q / h_f \tag{2}$$

and noting that k_f and t_f are assumed to be uniform throughout the domain, permits the fin equation for the fin region to be written as

$$\frac{\partial^2 T_1}{\partial x^2} + \frac{\partial^2 T_1}{\partial y^2} - \frac{h_f}{k_f t_f}(T_1 - T_s) = 0; \quad \text{fin} \tag{3}$$

while an analogous procedure for the energy removal piping material results in the equation

$$\frac{\partial^2 T_2}{\partial x^2} + \frac{\partial^2 T_2}{\partial y^2} - \frac{h_p}{k_p t_p}(T_2 - T_p) = 0; \quad \text{piping} \tag{4}$$

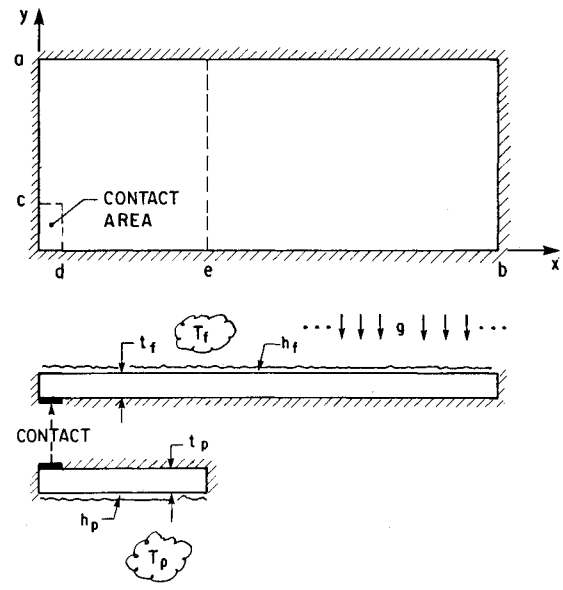

Fig. 2 Problem model geometry.

where it is noted that the pipe is modeled as an equivalent flat plate of appropriate planform.

The boundary conditions for the above two partial differential equations are given by

Fin:

$$\left.\frac{\partial T_1}{\partial x}\right|_{x=0} = 0 \tag{5a}$$

$$\left.\frac{\partial T_1}{\partial y}\right|_{y=0} = 0 \tag{5b}$$

$$\left.\frac{\partial T_1}{\partial x}\right|_{x=b} = 0 \tag{5c}$$

$$\left.\frac{\partial T_1}{\partial y}\right|_{y=a} = 0 \tag{5d}$$

Piping:

$$\left.\frac{\partial T_2}{\partial x}\right|_{x=0} = 0 \tag{6a}$$

$$\left.\frac{\partial T_2}{\partial y}\right|_{y=0} = 0 \tag{6b}$$

$$\left.\frac{\partial T_2}{\partial x}\right|_{x=e} = 0 \tag{6c}$$

$$\left.\frac{\partial T_2}{\partial y}\right|_{y=a} = 0 \tag{6d}$$

Contact:

$$T_1 = T_2 = T_c \quad \text{over} \quad 0 < x < d,\ 0 < y < c \tag{7a}$$

$$\frac{\partial^2 T_c}{\partial x^2} + \frac{\partial^2 T_c}{\partial y^2} - \frac{h_f}{(k_f t_f + k_p t_p)}(T_c - T_s) - \frac{h_p}{(k_f t_f + k_p t_p)}(T_c - T_p) = 0 \tag{7b}$$

In the latter equation, Eq. (7b), it is recognized that the energy transport within the contact area will occur in both the fin and the plate material and that convection occurs both to the sol-air temperature T_s and the energy removal temperature T_p.

The above equations and boundary conditions are nondimensionalized by introducing the following nondimensional variables:

$$x^* = x/a \tag{8a}$$

$$y^* = y/a \tag{8b}$$

$$\theta = \frac{T - T_p}{T_s - T_p} \tag{8c}$$

Further, the Biot modulus and nondimensional thickness are defined according to

$$Bi = ht/k \tag{9}$$

and

$$t^* = t/a \tag{10}$$

Using these definitions, the governing equations become

$$\frac{\partial^2\theta_1}{\partial x^{*2}} + \frac{\partial^2\theta_1}{\partial y^{*2}} - \frac{Bi_f}{t_f^{*2}}\theta_1 = \frac{-Bi_f}{t_f^{*2}} \tag{11}$$

$$\frac{\partial^2\theta_2}{\partial x^{*2}} + \frac{\partial^2\theta_2}{\partial y^{*2}} - \frac{Bi_f}{t_p^{*2}}\theta_2 = 0 \tag{12}$$

and the boundary conditions become

Fin:

$$\left.\frac{\partial\theta_1}{\partial x^*}\right|_{x^*=0} = 0 \tag{13a}$$

$$\left.\frac{\partial\theta_1}{\partial y^*}\right|_{y^*=0} = 0 \tag{13b}$$

$$\left.\frac{\partial\theta_1}{\partial x^*}\right|_{x^*=\beta} = 0 \tag{13c}$$

$$\left.\frac{\partial\theta_1}{\partial y^*}\right|_{y^*=1} = 0 \tag{13d}$$

Piping:

$$\left.\frac{\partial\theta_2}{\partial x^*}\right|_{x^*=0} = 0 \tag{14a}$$

$$\left.\frac{\partial\theta_2}{\partial y^*}\right|_{y^*=0} = 0 \tag{14b}$$

$$\left.\frac{\partial\theta_2}{\partial x^*}\right|_{x^*=\zeta} = 0 \tag{14c}$$

$$\left.\frac{\partial\theta_2}{\partial y^*}\right|_{y^*=1} = 0 \tag{14d}$$

Interface:

$$\theta_1 = \theta_2 = \theta_c; \quad 0 < x^* < \delta, \quad 0 < y^* < \gamma \tag{15a}$$

$$\frac{\partial^2\theta_c}{\partial x^{*2}} + \frac{\partial^2\theta_c}{\partial y^{*2}} - \left(\frac{Bi_f}{t_f^{*2}(1+1/\kappa)} + \frac{Bi_p}{t_p^{*2}(\kappa+1)}\right)\theta_c = -\frac{Bi_f}{t_f^{*2}(1+1/\kappa)}; \quad 0 < x^* < \delta, \quad 0 < y^* < \gamma \tag{15b}$$

To summarize, there are many problem parameters on which the solution, in general, will depend. Functionally this dependence can be written as

$$\theta = \theta(Bi_f/t_f^{*2}, Bi_p/t_p^{*2}, \beta, \zeta, \delta, \gamma, \kappa, x^*, y^*) \tag{16}$$

where

$$\kappa = k_f t_f / k_p t_p \tag{17}$$

has been defined and the nondimensional distances, β, ζ, δ, and γ, are as illustrated in the nondimensional problem domain of Fig. 3.

Fin Performance

When presenting the thermal performance characteristics of fins, it is customary to present the fin efficiency η_f which is defined as the heat rate divided by the rate that would be achieved if the fin were *isothermal* at its base temperature. In solar collection applications, however, the collection efficiency η_c compares the actual energy transfer rate to the rate at which the radiative energy is *incident* upon the surface of the fin. To examine the influence of geometric parameters related to weld size, however, it is better to remove the direct dependence of the collection efficiency on the absorptivity of the fin surface. Therefore, a collector transfer efficiency, η_t, will be introduced that compares the actual energy transfer rate to the rate at which incident energy is radiatively *absorbed*. These efficiencies are related, however, according to the following relations:

$$\eta_c = \alpha\eta_t \tag{18}$$

$$\eta_f = (1 - \theta_f)\eta_t \tag{19}$$

where θ_f is the nondimensional value of the actual fluid (not sol-air) temperature with which the fin surface interacts convectively.

The efficiency to be presented in this paper is the collector transfer efficiency, η_t. Mathematically, the collector transfer coefficiency can be expressed as

$$\eta_t = -\int\int_{\text{fin}} h_f(T - T_s)\,dx\,dy \Big/ \int\int_{\text{fin}} \alpha q\,dx\,dy \tag{20}$$

Further noting that α and q are constant, and expressing η_t in terms of nondimensional parameters, we obtain

$$\eta_t = \frac{1}{(1-\theta_f)}\left\{1 - \frac{1}{A_f^*}\int\int_{\text{fin}} \theta\,dx^*\,dy^*\right\} \tag{21}$$

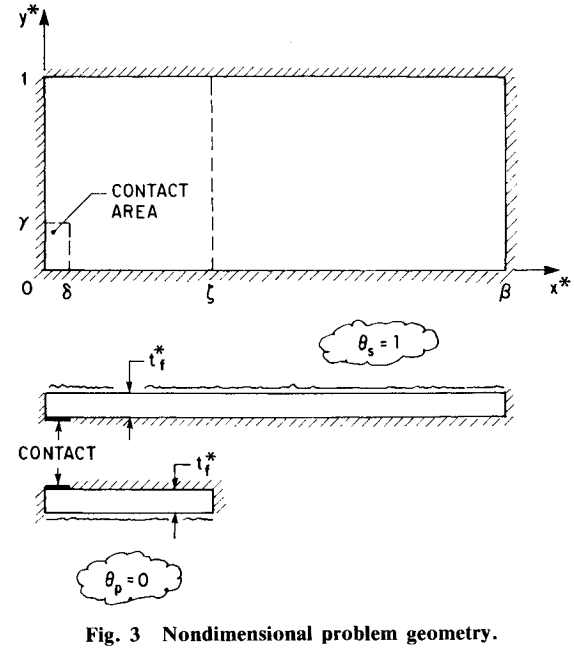

Fig. 3 Nondimensional problem geometry.

where

$$\alpha q/h_f = T_f - T_s \tag{22}$$

and

$$A_f^* = \int \int_{\text{fin}} dx^* dy^* \tag{23}$$

have been employed. The above efficiency of energy transfer depends upon the parameters indicated by Eq. (16), with the exception of x^* and y^*, and, in addition, depends upon the value of θ_f. Thus, an additional parameter has been introduced through the definition of the efficiency. To minimize the impact of this additional parameter, and to emphasize the dependence of the fin performance of the weld characteristics, we introduce the relative performance ratio (RPR), which relates the actual transfer efficiency to that which would be experienced if the weld were continuous, i.e., $\gamma = 1$, and if the heat transfer were therefore one-dimensional.

Therefore, the relative performance ratio is defined according to

$$\text{RPR} = \eta_t / \eta_{t_{1-D}} \tag{24}$$

which removes the dependence on θ_f. This definition has the further benefit in that the relative performance expressed in this manner presents the influence of geometry, weld size and shape, and convective parameters on the relative performance, and that this relative performance is unique, independent of which definition of actual efficiency is employed. The dependence of the RPR can be expressed functionally as

$$\text{RPR} = \text{RPR}\ (Bi_f/t_f^{*2},\ Bi_p/t_p^{*2}, \beta, \zeta, \delta, \gamma, \kappa) \tag{25}$$

which still contains a significant number of parameters. The list of parameters will be reduced on the basis of physical arguments when the numerical results are presented.

Numerical Solution

The finite element method was employed to solve the overall problem. Each component, the fin and the piping, was subdivided into a system of two-dimensional finite elements. The Galerkin finite element procedure was employed to solve the complete coupled problem with linear, quadrilateral, isoparametric finite elements used in the discrete approximation to the continuum problem.

In order to study the effect of the various geometric parameters of the problem, a grid generator was constructed which provided a nonuniform distribution of elements and element sizes. This was necessary to capture the detailed distortion of the thermal field in the vicinity of the actual contact while not being excessively wasteful, from a computational point of view, in the distant regions of the fin where the thermal field is highly regular. The fin and piping grids were constructed independently with the necessary essential criterion being that over the region of contact the planform of the overlaying elements must be common to both the fin and piping. The method of establishing element sizing throughout the domain was based on the size of the weld itself. A fine mesh was established, based on weld size, throughout the entire piping domain. A replica of this distribution was then overlayed on the fin portion of the domain and the remaining section of fin toward its outer edge was subdivided into coarser elements; these elements being a multiple of the finer element size in the x direction. In this way, a fine grid was established in both the fin and piping in the vicinity of the weld, where it is important to capture the details of the constricting thermal field. Efforts were made in the numbering scheme to minimize bandwidth and hence solution costs. A direct solution algorithm was employed to effect the solution.

The code was validated initially through application to three test problems whose geometry conforms to that of the actual problem. These three test problems are all cases for which the weld is continuous and, through appropriate selection of problem parameters, represent three different one-dimensional problems for which an analytic solution can be found. These test configurations are shown in Fig. 4. In all three cases, excellent agreement with the analytic solution was obtained with errors well below 1%. In addition, a convergence study was performed for a highly constricting case of small weld size ($\gamma = 0.2$, $\delta = 0.08$). Element distributions ranging from 173 to 582 elements were examined with the total change in efficiency from the coarsest to the finest mesh being approximately 0.5%. The coarser mesh allocation system was employed for the subsequent parametric evaluations with frequent spot checks performed on specific cases with a finer mesh in order to maintain a local assessment of convergence. It is estimated, on the basis of the above studies and spot checks, that the solutions presented for the transfer efficiency are within 1%.

Results

The relative performance ratio relates the actual efficiency to the one-dimensional, continuous weld efficiency. This requires, therefore, that the one-dimensional efficiency be available so that actual efficiencies can be determined, if desired, in addition to the influence of weld geometry on the performance. As a result, the one-dimensional efficiency will be presented first. However, it is instrumental before proceeding, to reduce, to the extent possible, the number of parameters on which the efficiency depends, without significantly restricting the utility or applicability of the results.

With respect to presenting the one-dimensional efficiency, the dependence on θ_f appears only in the premultiplying fac-

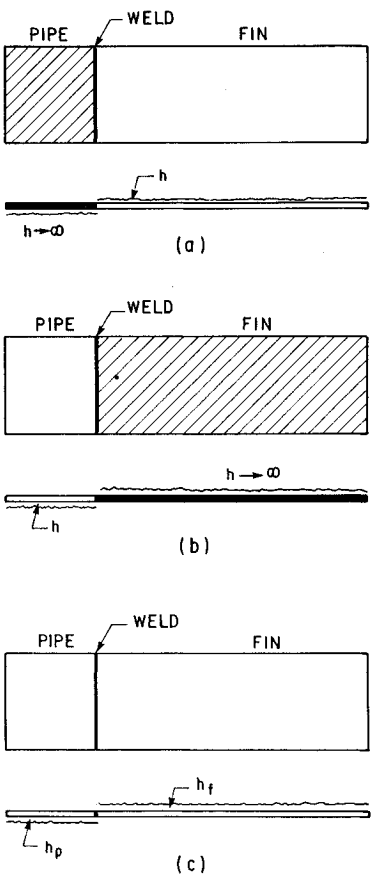

Fig. 4 One-dimensional test problems.

tor of Eq. (21). Thus, we will present the product $\eta_t(1-\theta_f)$, which is given by

$$\eta_t(1-\theta_f)=\left\{1-\frac{1}{A_f^*}\int\int_{\text{fin}}\theta dx^* dy^*\right\} \tag{26}$$

and, in this form, the right-hand side does *not* depend on θ_f.

Second, the restriction will be made to situations in which Bi_p/t_p^{*2} is large. This is reasonable in consideration of forced convection flow in the energy removal piping with natural convection over the fin surface under typical conditions. Further, as can be argued from a physical basis, and was supported by performing actual numerical experiments, this restriction renders the parameters ζ and κ ineffectual insofar as their impact on both the efficiency and relative performance ratio is concerned. Testing indicated that, with large values of Bi_p/t_p^{*2}, the influence of ζ and κ on the relative performance ratio was only a fraction of 1%. These tests included a wide range of values of ζ and κ.

Under the above conditions, the relative performance ratio can be expressed effectively in the form

$$\text{RPR}=\text{RPR}(Bi_f/t_f^{*2},\beta,\delta,\gamma); \qquad Bi_p/t^{*2}\to\infty \tag{27}$$

while the one-dimensional efficiency will not retain a dependence on γ. Moreover, for the one-dimensional case, the section width a is inappropriate for normalization, and the length b is more suitable. Indeed, in the one-dimensional standard fin analyses the influence of the Biot modulus and fin length appear as a single parameter. Making the necessary modifications to reflect these realizations, the form of the one-dimensional efficiency is expected to be

$$\eta_{t_{1-D}}(1-\theta_f)=f(\phi,\delta) \tag{28}$$

where

$$\phi=\beta^2 Bi_f/t_f^{*2} \tag{29}$$

reflects the expected one-dimensional behavior. For practical weld sizes the influence of δ is further expected to be relatively weak.

Both of the above-described expectations are supported by the results of numerical experiments. These results, presented in Fig. 5, demonstrate the weak influence of δ for $\delta=0.02$ and 0.10. Further, the curves presented are composite curves consisting of different sets of overlapping numerical data corresponding to differing combinations of β and Bi_f/t_f^{*2}. Their representation on a single curve for a fixed δ strongly supports the expected dependence on β and Bi_f/t_f^{*2} only in combination through ϕ as defined by Eq. (29). Therefore, the plot presented in Fig. 5 can be used to determine the one-dimensional efficiencies for use in combination with the relative performance ratios to be presented below. Equations (18) and (19) can be used to relate the different efficiencies to each other based on their definitions. It is further observed that the one-dimensional efficiencies as plotted behave as expected; that is, for small values of ϕ the efficiencies approach 100%, while for increasing values of ϕ the efficiency is degraded. This, of course, is based on the conventional definition of fin efficiency. Through combination of Eqs. (18) and (19), however, the actual collection efficiency η_c can be expressed in the form

$$\eta_c=\frac{\alpha}{(1-\theta_f)}\eta_f \tag{30}$$

which shows the direct dependence of collection efficiency on the fin surface absorbtivity and the inverse complementary dependence on the fin environmental fluid temperature, in nondimensional terms, θ_f.

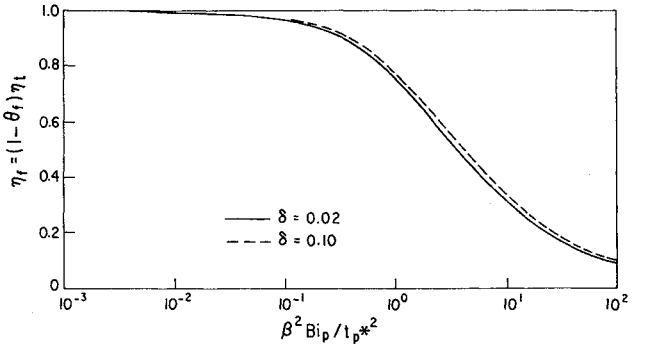

Fig. 5 One-dimensional fin efficiency.

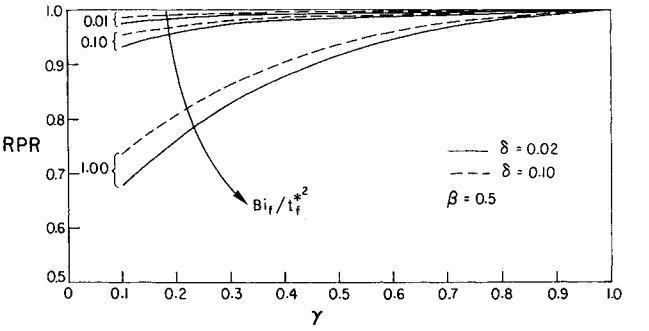

Fig. 6 Relative performance ratio for $\beta=0.5$.

The relative performance ratio is presented in Figs. 6-8 for the actual two-dimensional situation for three different nondimensional fin lengths, β. These curves present the relative performance ratio as a function of γ, the weld length along the pipe axis, for various values of Bi_f/t_f^{*2}. The dependence of the relative performance ratio on the weld width δ is relatively weak for the typical values considered. This is an expected weak dependence. The dependence on both Bi_f/t_f^{*2} and γ, however, is more severe as also is expected. All of these figures indicate a degradation in performance through a reduction in the RPR as the weld length γ is decreased. This corresponds directly to the increased thermal resistance resulting from the necessary constriction of the heat flow as it passes through the limited region of contact. At low values of Bi_f/t_f^{*2} the influence of the finite weld size is considerably less than that which is felt at higher values. This is due to the fact that at low values of Bi_f/t_f^{*2}, the performance of the fin is dominated by the resistance of the surface convective layer. As the fin length is increased, however, and the fraction of the total resistance that can be identified with the surface layer decreases, the influence of γ becomes more pronounced even at the lower value of Bi_f/t_f^{*2}. This is evidenced by the increased dependence on γ as β is increased from 0.5 to 2.0 to 6.0 in Figs. 6-8.

As the convective resistance is decreased, through increasing Bi_f/t_f^{*2}, the dependence on γ increases. Indeed, the degradation in performance is highly significant for $Bi_f/t_f^{*2}=1.0$. Further, at the higher values of Bi_f/t_f^{*2}, the fin system becomes thermally long sooner than for lower values. This can be seen by comparing the curves for $Bi_f/t_f^{*2}=1.0$ for $\beta=2$ and 6.0. These particular curves effectively overlay each other indicating that the additional length, for this larger value of Bi_f/t_f^{*2}, has little effect on the fin relative performance. Indeed, for these cases the fin efficiency itself is quite low, and the cause of the continued decrease in the conventional actual efficiency is due to the increasing value of ideal fin heat transfer in the denominator while the actual heat-transfer rate has reached an asymptotically limiting

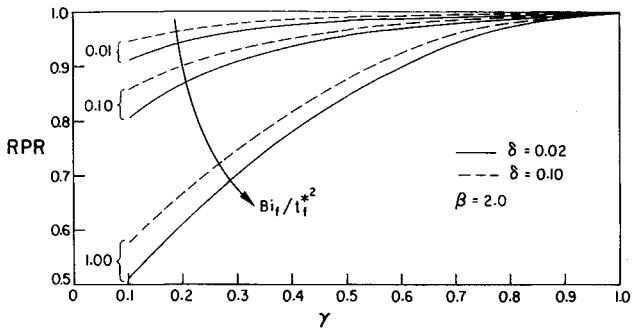

Fig. 7 Relative performance ratio for $\beta = 2.0$.

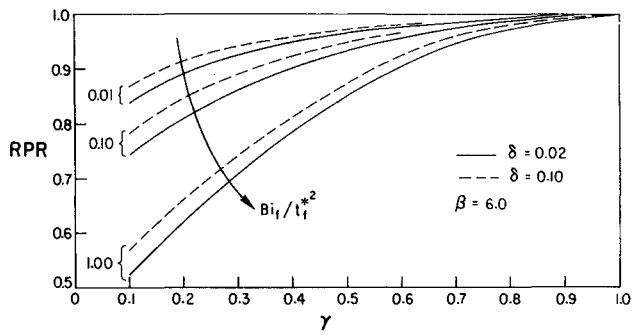

Fig. 8 Relative performance ratio for $\beta = 6.0$.

value. This asymptotic value is reached at shorter lengths as the convective exchange coefficient is increased. For the lower values of Bi_f/t_f^{*2}, there remains a significant dependence of the performance characteristics as the fin length is increased from $\beta = 2$ to 6. It is apparent from these figures that there is a significant degradation of performance as the weld size is decreased, and that this degradation depends strongly on the value of Bi_f/t_f^{*2}. For the shorter fins, however, at lower values of Bi_f/t_f^{*2}, the shorter weld lengths do not influence the fin performance significantly.

A second realization, in addition to the above performance characteristics, has surfaced as a result of this investigation. This realization, as can be argued on a physical basis, is that, in the constriction region of this two-dimensional constriction problem, the resistance within the conducting members is not controlled by the actual area of contact, but, rather, by the perimeter of the weld region. In the two-dimensional configuration, of course, the area through which the heat flow occurs is determined as the product of the weld perimeter and the fin thickness so that in this sense it is indeed the *flow area* in the constriction zone that dominates the determination of the performance. This is exemplified by reference to Fig. 9. In this figure, six different weld geometries, albeit all rectangular, are illustrated. Each of these rectangular contacts, labeled as cases 1-6, have a common value for their perimeter length. The figure corresponds to $Bi_f/t_f^{*2} = 0.1$ and $\beta = 2.0$ and it is noted that the contact planform area varies by as much as a factor of 7.5, from 0.012 to 0.09, in nondimensional terms. However, the value of the fin efficiency, $\eta_f = (1-\theta_f)\eta_t$, varies by less than 2% considering all configurations presented. Further, these configurations are markedly different, as can be seen by comparing cases 1 and 6, and yet the resulting efficiencies are effectively the same. Thus it would be reasonable to suggest that the results presented in this paper could be extended to weld geometries other than rectangular, provided that the extension is made with the constraint that contact perimeter

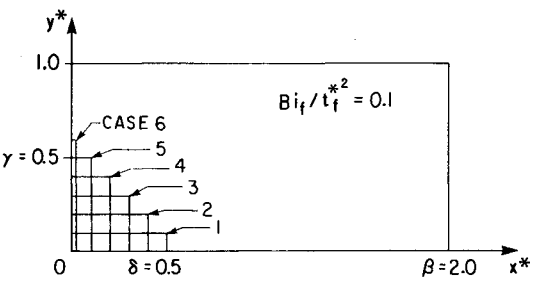

CASE	δ	γ	δ + γ	δ × γ	η_f [%]
1	0.5	0.1	0.6	0.05	87.2
2	0.4	0.2	0.6	0.08	88.1
3	0.3	0.3	0.6	0.05	88.1
4	0.2	0.4	0.6	0.08	87.6
5	0.1	0.5	0.6	0.05	86.6
6	0.02	0.6	0.62	0.012	88.3

Fig. 9 Configuration study illustrating the importance of weld perimeter.

is constant throughout the extension. The error incurred through such an extrapolation would appear to be on the order of only several percent. Indeed, this is, a powerful capability and will permit direct application of the results presented in this paper to arbitrary weld shape situations provided the weld perimeter is employed in performing the extrapolation.

Conclusions

The problem addressed herein has been that of determining the influence of weld size on the degradation of performance of fin systems from their continuous weld performance. The utility of employing a discontinuous weld-fastening procedure has significant implications on the economics of fabrication of such systems and concern regarding such economic considerations has already been voiced by the solar collector industry. Heretofore, the problem itself has not been addressed.

The problem geometry has been described and the mathematical formulation of the problem has been presented in detail. The governing equations and boundary conditions were then nondimensionalized to provide greater universality of application of the results. This procedure revealed a large number of parameters intrinsic to the problem specification. This list was substantially reduced in recognition that practical configurations will experience a highly convecting flow situation along the pipe wall when compared to that experienced by the fin surface. A large Biot modulus was employed for the tube side, which effectively makes the tube inner wall isothermal, and it was demonstrated that the dependence on ζ thereby becomes insignificant. The primary dependence of interest, that of γ and δ, however, was preserved under this restriction. In addition, it was observed that the magnitude of the fin side Biot modulus, through Bi_f/t_f^{*2}, has a significant influence on the dependence of fin efficiency on γ and δ.

Relations have been presented that relate the differently defined efficiencies, collection, conventional, and energy transfer efficiencies, and thereby enable the results presented to be used in varying formats. Further, a novel concept of a relative performance ratio, RPR, has been introduced so that the influence of the two-dimensionality on fin performance, through γ and δ in this specific situation, can be readily assessed. This performance ratio is independent of the par-

ticular definition employed for the fin efficiency and, therefore, the results presented in this form are applicable universally. This performance ratio relates the two-dimensional efficiency to the continuous weld, one-dimensional efficiency, and it is expected that this concept will be useful in future two-dimensional fin analyses.

New results have been presented, in terms of the relative performance ratio, for the fin problem examined herein. These results definitively illustrate the influence of weld geometry on performance and, therefore, will be useful in designing discontinous weld fin systems. It was observed that the performance of the fin system can be degraded significantly through the introduction of small weld areas, particularly for large Biot moduli on the fin surface. In order to use these relative performance ratios directly, a plot of the corresponding one-dimensional efficiency has been provided.

Further, it was found that the controlling factor in the fin efficiency or the relative performance ratio was the perimeter of the weld area. This was dramatically demonstrated through consideration of six drastically different weld configurations, each of which entailed the same weld perimeter although the embodied weld areas varied by a factor of 7.5. It was observed that these dramatically different contact configurations, having a common perimeter length, resulted in efficiencies differing by less than 2%. This was indeed a powerful realization and will permit the results presented herein to be used for weld configurations having significantly different weld shapes.

Acknowledgments

The authors thank the Natural Sciences and Engineering Research Council of Canada for their financial support of this project in the form of an operating grant to G.E. Schneider. The authors also express their appreciation to Dr. K.G.T. Hollands for initially suggesting this problem and for noting the need for its resolution.

References

[1]Schneider, G.E., "Thermal Resistance of Circular Cylinder Cross-Sections with Convective and Flux Prescribed Boundaries," *AIAA Journal,* Vol. 22, No. 6, June 1984, pp. 857-860.

[2]Shapiro, T., "Design of a Double Wall Exchanger for Hazardous Service," *Chemical Engineering Progress Symposium Series,* Vol. 95, No. 92, 1959, pp. 64-69.

[3]Oliveira, H.Q. and Forslund, R.P., "The Effect of Thermal Constriction Resistance in the Design of Channel-Plate Heat Exchangers," *ASME Journal of Heat Transfer,* Vol. 95, Ser. C, Aug. 1974, p. 292.

[4]Schneider, G.E., Yovanovich, M.M., and Cane, R.L.D., "Thermal Resistance of a Convectively Cooled Plate with Nonuniform Applied Flux," *Journal of Spacecraft and Rockets,* Vol. 17, Aug. 1980, pp. 372-376.